Cotunnelling versus sequential tunnelling in Coulomb blockade metallic double quantum dot structures

2006 J. Phys.: Condens. Matter 18 2729

(http://iopscience.iop.org/0953-8984/18/9/010)

INSTITUTE OF PHYSICS PUBLISHING JOURNAL OF PHYSICS: CONDENSED MATTER

J. Phys.: Condens. Matter **18** (2006) 2729–2740 doi:10.1088/0953-8984/18/9/010

Cotunnelling versus sequential tunnelling in Coulomb blockade metallic double quantum dot structures

V Duc Nguyen, V Hung Nguyen and V Lien Nguyen[1]

Theoretical Department, Institute of Physics, VAST, PO Box 429, Bo Ho, Hanoi 10000, Vietnam

E-mail: nvlien@iop.vast.ac.vn

Received 21 November 2005, in final form 23 January 2006
Published 17 February 2006
Online at stacks.iop.org/JPhysCM/18/2729

Abstract

The cotunnelling is systematically studied in comparison to sequential tunnelling in Coulomb blockade metallic double quantum dot structures, using the standard master equation approach. In the case of zero gate voltage, we are able to derive analytical expressions of threshold voltages for both tunnelling processes: $V_{\rm th}^{(s)}$ for the sequential tunnelling and $V_{\rm th}^{(2)}$ for the lowest-order inelastic macroscopic quantum tunnelling (cotunnelling). Taking into account the gate and temperature effects, numerical solutions of the master equation show that an increase of the inter-dot capacitance leads to a decrease of the ratio $V_{\rm th}^{(2)}/V_{\rm th}^{(s)}$ and at the same time to a decrease of cotunnelling conductance compared to the sequential one. An oscillation of cotunnelling conductance is observed in classical Coulomb blocked regions. In comparison with the sequential tunnelling conductance spectroscopy, the peak height of cotunnelling conductance is about three orders of magnitude smaller and the peak spacing distribution is far from regular. Increase of temperature raises the current and destroys the Coulomb gap. Its relative influence is more important at lower bias.

(Some figures in this article are in colour only in the electronic version)

1. Introduction

The Coulomb blockade (CB), observed widely in quantum dot (QD) structures, has attracted great attention from both fundamental physics and technological applications. At the CB regime in current–voltage (I–V) characteristics there exists a gap of $V < V_{\rm th}^{(s)}$, where the current associated with the sequential electron tunnelling strictly vanishes. The threshold voltage $V_{\rm th}^{(s)}$ is the most important quantity, characterizing the CB phenomenon. This quantity has been analytically evaluated for some simple structures [1], e.g. single QD structures or arrays of identical QDs, using the so-called Orthodox theory [2]. It was however predicted

[1] Author to whom any correspondence should be addressed.

early that taking into account higher-order electron tunnelling processes (macroscopic quantum tunnelling—q-MQT) the current could be finite even at $V < V_{\mathrm{th}}^{(s)}$ [3]. There are two kinds of q-MQT: the inelastic process associated with the simultaneous tunnelling of different electrons through different junctions, and the elastic one, where one electron tunnels across two or several junctions. While the former process gives a major contribution to the total q-MQT current in metallic or large semiconductor QDs, where the energy spectrum is essentially continuous or many levels contribute to tunnelling, the latter becomes important in small QDs, where the energy levels are well separated. In this paper, since the object of study is metallic QDs we will be interested in only the inelastic process, which for short will be called the cotunnelling.

In the theory of quantum transport through CB metallic QDs, developed by Schoeller and Schön [4], the sequential tunnelling (ST) and cotunnelling (CT) can be respectively described by the lowest-order and the second-order perturbation with respect to the parameter $R_{\mathrm{Q}}/R_{\mathrm{t}}$, where $R_{\mathrm{Q}} = h/e^2$ is the quantum resistance and R_{t} is the tunnelling resistance of a single tunnelling junction. In this theory the range of parameter $R_{\mathrm{Q}}/R_{\mathrm{t}}$ and of temperature, where the CT may be dominant, was also well identified. Experimentally, the CT has been measured in various metallic [5–7] and semiconductor [8–10] QD structures. Though the CT current is much smaller than that due to the ST, it basically destroys the classical CB effect, giving rise to a limitation to the accuracy of single electron devices.

Generally, in a linear array of N junctions, regarding the number of electrons involved in one CT act, the CT can be seen as consisting of n-electron processes, where n can be from 2 to N. While the contribution from each process to the total CT current decreases quickly with increasing the order n, analytical calculations can be done only for the highest-order $n = N$, when all the junctions are equivalent in the sense that each of them experiences simultaneously a 'partial' single electron tunnelling. For this process the zero temperature CT rate has the form [3]

$$\Gamma_N \propto V^{2N-1} \prod_{i=1}^{N} (R_{\mathrm{Q}}/R_{\mathrm{t}i}), \tag{1}$$

where V is the applied voltage and $R_{\mathrm{t}i}$ is the tunnelling resistance of i-junction. The I–V characteristics deduced from this rate expression describes well experimental data for linear arrays of two and three metallic tunnel junctions [5, 7]. On the other hand, because the range of bias voltages, where the n-electron process is most favourable, moves down as n increases it is reasonable to assume that for each n-electron process there exists a threshold voltage $V_{\mathrm{th}}^{(n)}$, and on the whole, for a given measurement sample, $V_{\mathrm{th}}^{(s)} > V_{\mathrm{th}}^{(2)} > \cdots > V_{\mathrm{th}}^{(N-1)} > V_{\mathrm{th}}^{(N)} = 0$. Qualitatively, the tunnelling phenomenon is thus well understood. However, currently, its quantitative description is mostly limited to single QD structures. Recently, the double quantum dot structures have been strongly suggested as the most prospective candidate for a solid state qubit [11–13], and therefore have become a very attractive object of both experimental [14] and theoretical [15–18] investigations. In the structure where two quantum dots are embedded between three tunnel junctions (figure 1(a)), two dominant tunnelling processes are the ST and the two-electron cotunnelling (2ECT). Two corresponding threshold voltages are $V_{\mathrm{th}}^{(s)}$ and $V_{\mathrm{th}}^{(2)}$, while $V_{\mathrm{th}}^{(3)}$ is already zero (following (1)). The aim of the present work is, using the standard master equation approach, to derive exact expressions of the thresholds, $V_{\mathrm{th}}^{(s)}$ and $V_{\mathrm{th}}^{(2)}$, for this configuration of metallic double quantum dot structures (MDQDSs) without gate and to numerically calculate the I–V characteristics for both ST and 2ECT, taking into account the gate and temperature effects. The obtained results give a quantitative description of how the 2ECT is important, compared to the ST, in devices with different parameters. We neglect the higher-order three-electron tunnelling process, which becomes important only at lower bias

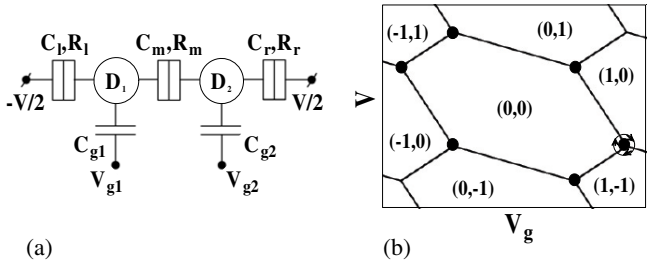

Figure 1. (a) Equivalent circuit diagram of the MDQDS under study; (b) illustrative diagram used to evaluate threshold voltages (see section 3).

voltages and at lower temperatures. Also, we do not consider the structures where two QDs are coupled in parallel, as discussed, for example, in [12, 18].

The paper is organized as follows. Section 2 is devoted to formulating the problem and presenting fundamental expressions. In section 3 we derive exact expressions for $V_{\rm th}^{(s)}$ and $V_{\rm th}^{(2)}$ in the case of zero gate voltages. These thresholds are identified as the voltages below which the ST (or 2ECT) is energetically blocked and over which there exists a finite current through the device. Numerical results of threshold voltages and conductance, taking into account the gate and temperature effects, are discussed in section 4. Lastly, a brief summary is given in section 5.

2. General consideration

The equivalent circuit diagram of the Coulomb blockade MDQDS studied is drawn in figure 1(a), where the gate with voltage $V_{\rm g1}$ (or $V_{\rm g2}$) is coupled to the dot D_1 (or D_2) via the gate capacitance $C_{\rm g1}$ (or $C_{\rm g2}$) and the bias voltage is applied symmetrically, $(-V/2, V/2)$. Within the framework of the Orthodox theory [2] the state of the system is entirely determined by the numbers of excess electrons in two dots, n and m. For a given (n, m)-state, the free energy of the system can be written as [19, 22]

$$F(n,m) = \frac{Q_1^2}{2C_l^*} + \frac{Q_2^2}{2C_r^*} + \frac{Q_1 Q_2}{C_m^*} + \frac{eV}{2}(n_l - n_r) - \frac{V^2}{8}(C_l + C_r) - \frac{1}{2}(C_{\rm g1}V_{\rm g1}^2 + C_{\rm g2}V_{\rm g2}^2). \tag{2}$$

Here $Q_1 = C_l V/2 - C_{\rm g2}V_{\rm g2} - ne$, $Q_2 = -C_r V/2 - C_{\rm g2}V_{\rm g2} - me$, $C_l^* = \Sigma/C_2$, $C_r^* = \Sigma/C_1$, $C_m^* = \Sigma/C_m$, $C_1 = C_m + C_{\rm g1} + C_l$, $C_2 = C_m + C_{\rm g2} + C_r$, $\Sigma = C_1C_2 - C_m^2$, and $n_l(n_r)$ is the number of electrons that have entered the structure from the left (right). Any electron transfer across junctions (l, m or r) results in a change in free energy F. The main electron tunnelling processes in MDQDSs of interest, as mentioned above, are ST and 2ECT.

For the ST, there are six possible electron transfers across three junctions to the right (+) or left (−). The change in free energy F associated with these STs can be easily deduced from equation (2) as

$$\begin{aligned}
\Delta F_l^{\pm}(n,m) &= e[(e/2 \mp Q_1)/C_l^* \mp Q_2/C_m^* \mp V/2] \\
\Delta F_m^{\pm}(n,m) &= e[(e/2 \pm Q_1)/C_l^* - (e \pm Q_1 \mp Q_2)/C_m^* + (e/2 \mp Q_2)/C_r^*] \\
\Delta F_r^{\pm}(n,m) &= e[(e/2 \pm Q_2)/C_r^* \pm Q_1/C_m^* \mp V/2].
\end{aligned} \tag{3}$$

The rate of an ST across any ν-junction, $\nu = l, m$ or r, is well known [2] for zero temperature:

$$\Gamma_\nu = \begin{cases} 0, & \Delta F_\nu \geqslant 0 \\ |\Delta F_\nu|/e^2 R_{t\nu}, & \Delta F_\nu < 0 \end{cases} \tag{4}$$

as well as finite temperatures:

$$\Gamma_\nu = (e^2 R_{t\nu})^{-1} \Delta F_\nu / [\exp(\Delta F_\nu / k_B T) - 1], \tag{5}$$

where ΔF_ν is the corresponding change in free energy defined in equation (3).

For the 2ECT, following Averin and Nazarov (AN) [3], we will neglect all the processes when two electrons tunnel across the same junction and when two electrons tunnel into or out of the same dot. Then, for MDQDSs under study, there are eight possible 2ECT transfers with the changes in free energy as follows:

$$\begin{aligned}
\Delta F_{lm}^{\pm\pm}(n,m) &= e[(e/2 \mp Q_2)/C_r^* \mp Q_1/C_m^* \mp V/2] \\
\Delta F_{lr}^{\pm\pm}(n,m) &= e[(e/2 \mp Q_1)/C_l^* - (e \mp Q_1 \pm Q_2)/C_m^* + (e/2 \pm Q_2)/C_r^* \mp V] \\
\Delta F_{lr}^{\pm\mp}(n,m) &= e[(e/2 \mp Q_1)/C_l^* + (e \mp Q_1 \mp Q_2)/C_m^* + (e/2 \mp Q_2)/C_r^*] \\
\Delta F_{mr}^{\pm\pm}(n,m) &= e[(e/2 \pm Q_1)/C_l^* \pm Q_2/C_m^* \mp V/2]
\end{aligned} \tag{6}$$

where the subscripts (e.g. lr) indicate the two junctions involved in the cotunnelling act, whereas the superscripts (e.g. $+-$) indicate the direction of partial tunnels across corresponding junctions. For example, $\Delta F_{lr}^{+-}(n,m)$ denotes the change in free energy F of the system at the state (n,m) due to the 2ECT, when two electrons tunnel simultaneously across l-junction to the right and r-junction to the left.

As for the 2ECT rate, AN [3] have derived both the zero and finite temperature expressions, but only for double junction systems. Extending the AN-calculating procedure to the MDQDS of interest we obtained the 2ECT rates as follows: for zero temperature

$$\Gamma_{\nu\mu} = \begin{cases} 0, & \Delta F_{\nu\mu} \geqslant 0 \\ (\hbar/12e^4\pi R_{t\nu} R_{t\mu})(1/\Delta F_\nu + 1/\Delta F_\mu)^2 \times \Delta F_{\nu\mu}^3, & \Delta F_{\nu\mu} > 0 \end{cases} \tag{7}$$

and for finite temperatures

$$\Gamma_{\nu\mu} = \frac{\hbar}{12e^4\pi R_{t\nu} R_{t\mu}} \left\{ \frac{1}{\Delta F_\nu} + \frac{1}{\Delta F_\mu} \right\}^2 \frac{\Delta F_{\nu\mu}(\Delta F_{\nu\mu}^2 + (2\pi k_B T)^2)}{\exp(\Delta F_{\nu\mu}/k_B T) - 1}. \tag{8}$$

Here ν and μ denote two junctions (with tunnelling resistances $R_{t\nu}$ and $R_{t\mu}$) involved in the CT act, ΔF_ν and ΔF_μ are the changes in free energy associated with two partial single electron tunnellings through these junctions considered separately (see equation (3)), and $\Delta F_{\nu\mu}$ is the difference in free energy between the initial and resulting states with respect to the CT event (see equation (6)). The expressions (7) and (8) have been obtained under the condition $|\Delta F_{\nu\mu}| \ll |\Delta F_\nu|, |\Delta F_\mu|$, implying the low bias voltages when the SET is blocked. To compare, respectively, these expressions, (7) and (8), with those, (12) and (14), in [3] we note that for the double junction structure studied in [3] the quantity $\Delta F_{\nu\mu}$ is nothing but eV.

Using expressions (3)–(5) for STs, or (6)–(8) for 2ECTs, in principle, we can solve the master equation or perform Monte Carlo simulations to get I–V characteristics at zero (using equation (4) or (7)) as well as finite temperatures (using equation (5) or (8)). For this paper, in fact, both calculation methods have been implemented; their results are however practically coincident in all cases of interest, and therefore, the only master equation (ME) is chosen to be discussed. Denoting $p(i)$ as the probability of the state $|i\rangle \equiv (n_i, m_i)$ of the system, the ME can be for short written in the matrix form (for details see the appendix):

$$\mathrm{d}\hat{p}(t)/\mathrm{d}t = \hat{M}\hat{p}(t), \tag{9}$$

where $\hat{p}(t)$ is the matrix of elements $p(i,t)$ and $\hat{M}$ is the evolution matrix of elements $M_{ij} = \Gamma(i \leftarrow j) - \delta_{ij}\sum_k \Gamma(k \leftarrow i)$ with $\Gamma(j \leftarrow i)$ being the net transition rate from $|i\rangle$ to $|j\rangle$, which is explicitly expressed in terms of tunnelling rates as shown in the appendix. Solving the ME (9) in the condition $\sum_i p(i,t) = 1$, one can further calculate the steady current, which is equal to the current through any of junctions, l, m or r:

$$I = e\sum_i [\Lambda_l^+ - \Lambda_l^-]p(i) \equiv e\sum_i [\Lambda_m^+ - \Lambda_m^-]p(i) \equiv e\sum_i [\Lambda^+ r - \Lambda_r^-]p(i), \tag{10}$$

where, taking into account 2ECTs, $\Lambda_l^+ = \Gamma_l^+(i) + \Gamma_{lm}^{++}(i) + \Gamma_{lr}^{++}(i) + \Gamma_{lr}^{+-}(i)$; $\Lambda_l^- = \Gamma_l^-(i) + \Gamma_{lm}^{--}(i) + \Gamma_{lr}^{--}(i) + \Gamma_{lr}^{-+}(i)$; $\Lambda_m^+ = \Gamma_m^+(i) + \Gamma_{lm}^{++}(i) + \Gamma_{mr}^{++}(i)$; $\Lambda_m^- = \Gamma_m^-(i) + \Gamma_{lm}^{--}(i) + \Gamma_{mr}^{--}(i)$; $\Lambda_r^+ = \Gamma_r^+(i) + \Gamma_{mr}^{++}(i) + \Gamma_{lr}^{++}(i) + \Gamma_{lr}^{-+}(i)$ and $\Lambda_r^- = \Gamma_r^-(i) + \Gamma_{mr}^{--}(i) + \Gamma_{lr}^{--}(i) + \Gamma_{lr}^{+-}(i)$. For the ST-current, in Λ-expressions all the 2ECT rates should be omitted.

In some simple cases, for example without gates at low applied bias and zero temperature as considered in [22, 23], the ME can be exactly solved, giving analytical expressions for I–V curves, and particularly, for threshold voltages as can be seen in the next section. With gates and at finite temperature, in general, the ME has to be solved numerically.

It should be here emphasized that the ME approach used is valid only in the strongly Coulomb blockade regime, when the charge (n,m)-states of the system are well defined. Such a regime has been identified in [4] with respect to the parameter R_Q/R_t and the temperature. For larger values of R_Q/R_t and at lower temperatures the coherent many-body transport may become considerable [12, 20, 21]. Experimentally, Franceschi *et al* [10] have shown that there really exists a range of temperature where the coherent correlations are still unimportant and the conduction is dominated by CT processes.

3. Threshold voltages: analytical expressions

Actually, the threshold voltages for both ST and 2ECT can be evaluated by solving the ME in the way as discussed recently in [22, 23]. In these works, we were able to exactly derive the I–V characteristics for the MDQDS of interest in the first Coulomb staircase region. The idea is that at low bias voltages there are only some available states, corresponding to the honeycomb cells immediately adjacent to the initial state (0, 0) in the stability diagram (see figure 1(b)), and therefore, the ME comes to be solved exactly. The net current appears when the bias voltage is high enough to create an electron transfer around a triple point associated with the state (0, 0). Then, in general, for the n-electron cotunnelling, the threshold can be defined as the voltage $V_{th}^{(n)}$, below which all the n-electron cotunnellings from the state (0, 0) are blocked and above which there appears a current through the device. The threshold voltages for STs and 2ECTs determined in this way of using the ME are respectively presented in sections 3.1 and 3.2, where for simplicity we consider the case of zero gate voltage, $V_{g1} = V_{g2} = 0$. The capacitances C_{g1} and C_{g2} can be then seen as the dot self-capacitances [24] and will be assumed to be equal, $C_{g1} = C_{g2} \equiv C_s$. The gate effect will be in detail examined by solving the ME numerically in the next section.

3.1. Sequential electron tunnelling threshold $V_{th}^{(s)}$

At zero temperature, as stated above, an electron transfer is energetically favourable only if it decreases the free energy F. Let us first consider the case of symmetrical MDQDSs when $C_l = C_r \equiv C$. Assuming that at zero bias voltage the system is in the state (0, 0), a finite bias voltage V (within the first Coulomb staircase) could cause an ST through some junction, resulting in a transition from this state to a nearest neighbour in the stability diagram (figure 1(b)). From

equation (3), with $n = m = 0$, $V_{g1} = V_{g2} = 0$, $C_{g1} = C_{g2} = C_s$, and $C_l = C_r = C$, we find that for bias voltages $V < V_t = e(C + C_s + C_m)/[(C + C_s)(2C + C_s + 2C_m)]$ all the changes in free energy are positive, i.e., all STs from the state $(0, 0)$ are strictly blocked. This means that the ST threshold $V_{th}^{(s)}$ we want to find must be not lower than V_t. To identify the voltage V_t as $V_{th}^{(s)}$ we have to show that at $V \geqslant V_t$ there exists at least one electron transition around a triple point of the cell $(0, 0)$ that opens a current through the device. In reality, as can be seen in equation (3), for bias voltages $V \geqslant V_t$, two quantities $\Delta F_l^+(0, 0)$ and $\Delta F_r^+(0, 0)$ are negative, implying that two transitions, $(0, 0)$ to $(1, 0)$ and $(0, 0)$ to $(0, -1)$, are energetically favourable. Further, starting from the state $(1, 0)$, we find that $\Delta F_r^+(1, 0) < 0$, showing a favour to the transition from $(1, 0)$ to $(1, -1)$. On the other hand, the transition from $(1, -1)$ back to $(0, 0)$ is always allowed, making an entire ST around the corresponding triple point. Thus, for $V \geqslant V_t$ there really exists a current through the device, and therefore, V_t is just the ST threshold voltage for the symmetrical MDQDS under study:

$$V_{th}^{(s)} = e(C + C_m + C_s)/[(C + C_s)(2C + 2C_m + C_s)]. \tag{11}$$

In the case of asymmetrical MDQDSs, using the same examining procedure as above with a little more complexity, the ST threshold $V_{th}^{(s)}$ can be also evaluated, but only under the following condition for device parameters (assuming $C_l > C_r$):

$$C_m \geqslant \frac{A + \{A^2 + 16(C_l - C_r)(C_l + C_r + 2C_s)(C_lC_r + C_lC_s + C_rC_s + C_s^2)\}^{1/2}}{4(C_l + C_r + 2C_s)}, \tag{12}$$

where $A = 2C_l^2 - 4C_lC_r - 2C_r^2 + C_lC_s - 7C_rC_s - 2C_s^2$. For instance, with $C_s = 0$ and $C_l = 2C_r$ this condition simply gives $C_m \geqslant C_r/2$. Under the condition (12) the ST threshold was found as

$$V_{th}^{(s)} = e(C_r + C_m + C_s)/[2C_lC_r + 2C_lC_m + C_s(2C_l + C_r + 2C_m + C_s)]. \tag{13}$$

The threshold voltage (13) turns into (11) in the particular case of symmetrical MDQDSs, when the condition (12) becomes trivial. Furthermore, if the self-capacitance C_s is set to be zero, the expressions (11) and (13) turn into the well-known expression [1]:

$$V_{th}^{(s)} = \min\{e/2C_l, e/2C_r\}. \tag{14}$$

The obtained results (11) and (13) show the role of each coupling capacitance in forming the Coulomb gap. The ST threshold is essentially defined by the largest capacitance in the device.

3.2. Two-electron cotunnelling threshold $V_{th}^{(2)}$

The threshold voltage $V_{th}^{(2)}$ can be determined in the way similar to that used above for STs. Certainly, one should here focus attention on only the range of bias voltages lower than $V_{th}^{(s)}$, where the STs are blocked. Assuming as above that at zero bias voltage the system is in the state $(0, 0)$, we have found from expressions (6) that there exists the voltage V_t, below which all the changes in free energy of equation (6) are positive, i.e., the initial state $(0, 0)$ is stable with respect to 2ECTs, while at $V \geqslant V_t$ the free-energy change $\Delta F_{lr}^{++}(0, 0)$ is negative, showing a favour to the transition from the state $(0, 0)$ to the state $(1, -1)$ caused by the 2ECT event, when one electron tunnels through the l-junction from the left and another electron tunnels through the r-junction to the right. Moreover, as noted above, the further transition from the state $(1, -1)$ back to the initial state $(0, 0)$ is always allowed, making a finite current across the structure. The voltage V_t found in this way is thus identified as the threshold for 2ECTs:

$$V_{th}^{(2)} = \frac{e(C_l + C_r + 2C_s)}{4C_lC_r + 2C_lC_m + 2C_rC_m + C_s(3C_l + 3C_r + 4C_m + 2C_s)}. \tag{15}$$

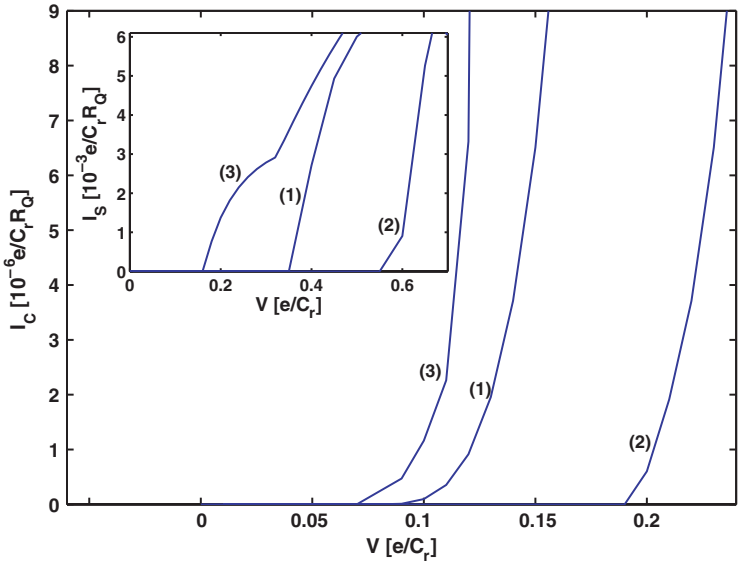

Figure 2. I–V characteristics calculated from numerical solutions of ME, taking into account 2ECTs, for the device with parameters $C_l = 1$, $C_m = 5$, $R_l = R_m = R_r = 10$, $C_{g1} = C_{g2} = 0.5$ and at various gate voltages, $V_g = 0$ (curve 1), 1.0 (curve 2), and 1.7 (curve 3). The temperature is zero. The I–V curves of STs for the same device at the same V_g are correspondingly presented in the inset for a comparison.

In the particular case of symmetrical MDQDSs with $C_l = C_r \equiv C$, this expression comes to have a simple form of $V_{\rm th}^{(2)} = e/(2C + 2C_m + C_s)$, which should be compared with the ST threshold (11). In the other particular case, when $C_s = 0$, the obtained 2ECT threshold voltage, $V_{\rm th}^{(2)} = e(C_l + C_r)/2(2C_lC_r + C_lC_m + C_rC_m)$, demonstrates the role of the inter-dot coupling capacitance C_m.

The expressions (11) (or (13)) and (15), together with (1), give the threshold voltages for all electron tunnelling processes of interest in MDQDSs under study. While the threshold $V_{\rm th}^{(3)}$ is already zero, the ratio between $V_{\rm th}^{(2)}$ and $V_{\rm th}^{(s)}$ mostly depends on the inter-dot capacitance C_m and the self-capacitance C_s. In the case of symmetrical structures this ratio is simply $V_{\rm th}^{(2)}/V_{\rm th}^{(s)} = (C + C_s)/(C + C_s + C_m)$, which increases with decreasing C_m and/or increasing C_s. The full curve of this ratio as a function of C_m is presented in figure 3, where the gate effect is also included.

4. Numerical results and discussion

To calculate I–V characteristics for both STs and 2ECTs, taking into account the gate and temperature effects, we have to solve the ME (9) (see the appendix for details), and then calculate the current (10) numerically. For each sample, two currents, I_S for STs alone and I_C with contributions from 2ECTs, are separately collected. In numerical calculations, for convenience, the elementary charge e, the quantum resistance $R_{\rm Q} \equiv h/e^2$, and the capacitance C_r are chosen as basic units. The voltage, the temperature, and the current are then measured in units of e/C_r, e^2/C_r, and $e^2/C_rR_{\rm Q}$, respectively.

In figure 2 we show, as an example, the I–V curves for 2ECTs of the device with parameters given in the figure. For a comparison, the low-bias part of I–V curves of STs for

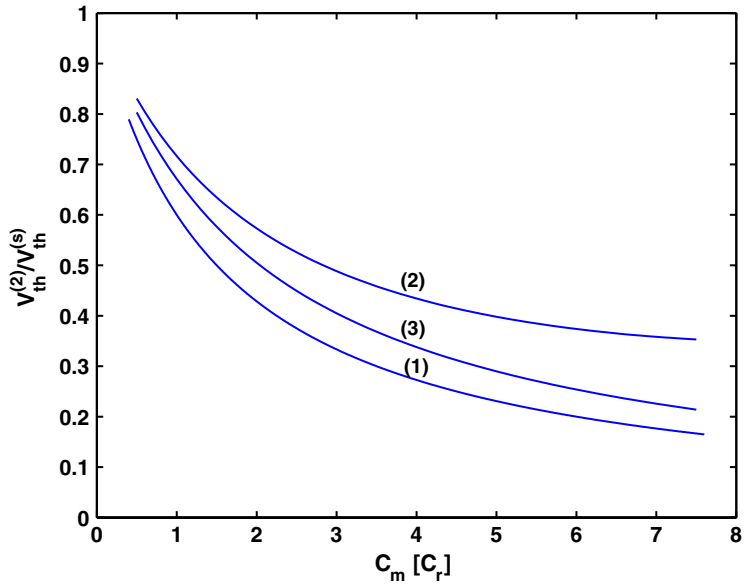

Figure 3. The ratio $V_{\rm th}^{(2)}/V_{\rm th}^{(s)}$ is plotted against the inter-dot capacitance C_m for the same device as that in figure 2 and with various gate voltages: $V_{\rm g} = 0$ (curve 1); 1.0 (curve 2); and 1.7 (curve 3).

the same device is also shown in the inset (the I–V curve of STs has been discussed in detail in [22]). Here as well as in other figures below, for simplicity, two gate voltages are always assumed to be equal, $V_{\rm g1} = V_{\rm g2} \equiv V_{\rm g}$. The calculations like those in this figure have been performed for devices with different inter-dot capacitances C_m and at different gate voltages $V_{\rm g}$.

From the I–V characteristics obtained, by comparing two curves, of STs and 2ECTs, for the same device and at the same $V_{\rm g}$, we can examine how the 2ECTs are important compared to the STs. In magnitude, the 2ECT current is always much smaller than the ST current (typically, $I_C/I_S \approx 10^{-3}$). For the threshold voltage, the ratio $V_{\rm th}^{(2)}/V_{\rm th}^{(s)}$ is sensitive to various device parameters: in particular, to the inter-dot capacitance C_m and the gate voltage $V_{\rm g}$.

Figure 3 shows the ratio $V_{\rm th}^{(2)}/V_{\rm th}^{(s)}$, plotted against C_m for three values of $V_{\rm g}$. Certainly, for the case of $C_{\rm g} = 0$, curve 1 can be directly produced from expressions (11) and (15). For any gate voltage $V_{\rm g}$, the ratio $V_{\rm th}^{(2)}/V_{\rm th}^{(s)}$ always decreases as C_m increases. In the limit of small C_m the 2ECT threshold approaches the ST one, implying a relative weakness of 2ECTs. In the opposite limit of large C_m, the threshold $V_{\rm th}^{(2)}$ becomes much smaller than $V_{\rm th}^{(s)}$, which implies a relatively important role of 2ECTs in smearing the classical Coulomb gap. Another interesting feature observed in figure 3 is an oscillation of the ratio $V_{\rm th}^{(2)}/V_{\rm th}^{(s)}$ as the gate voltage varies (compare curves 1–3 with $V_{\rm g} = 1,\ 1.2$ and 1.7, respectively). Such an oscillation of the ratio $V_{\rm th}^{(2)}/V_{\rm th}^{(s)}$ should be seen as a manifestation of a more general phenomenon: oscillation of the conductance with respect to the gate voltage, which is clearly demonstrated in figure 4.

Actually, figure 4 shows not only the well-known oscillation of the ST conductance (two peaks in the main figure), but also an oscillation of 2ECT conductance found in a classical blocked region (inset). Calculations performed for devices with different parameters show that in contrast to the ST conductance spectroscopy, for the 2ECT conductance, though the peaks are still of almost equal height, the peak spacing distribution is very far from regular, depending on device parameters. Another strong difference between the two conductance spectroscopies is the peak height. For the sample analysed in figure 4 the height of 2ECT-

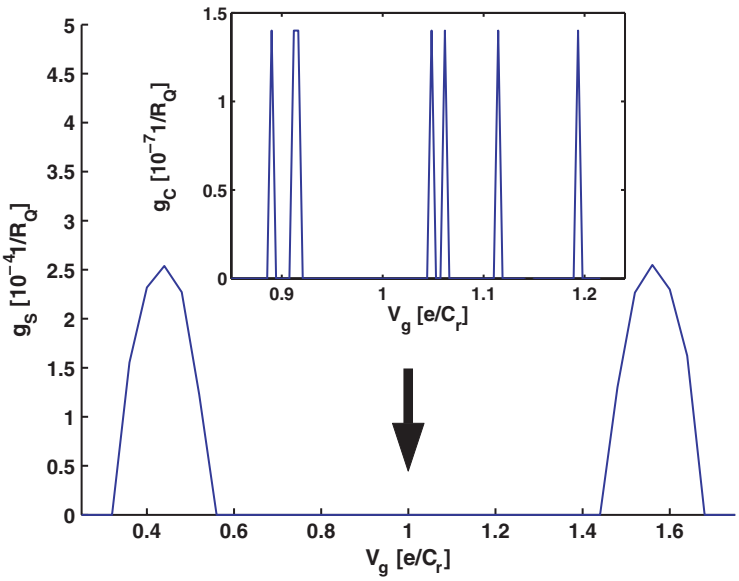

Figure 4. The typical conductance spectroscopy for 2ECTs (inset) which is found in a blocked region for STs (main figure). Note the difference in scale: the peak height for the 2ECT conductance is much smaller than that for the ST. The 2ECT conductance peak spacing distribution is far from regular.

conductance peaks is about in three orders of magnitude smaller than that of ST conductance peaks. We would like here to mention that Hanna *et al* [6], measuring tunnelling characteristics of a double metallic junction system, have reported on a similar value for the ratio of the two conductances. In fact, this ratio depends on device parameters. In particular, it should decrease with increasing tunnelling resistances. In figure 5, the ratio g_C/g_S is plotted against R_t for devices with all tunnelling resistances equal, $R_{tl} = R_{tm} = R_{tr} \equiv R_t$, and with different inter-dot capacitances C_m. Here, g_C and g_S respectively are typical values of the 2ECT and the ST conductance, determined at bias voltages close to corresponding thresholds. Clearly, the ratio g_C/g_S monotonically reduces as R_t becomes larger. And, interestingly, as can be seen in the inset of the figure, for any C_m it seems that $g_C/g_S \propto R_t^{-\gamma}$, where γ is almost independent of C_m and $\gamma \approx 1$.

Finally, we show in figure 6 the I–V characteristics, taking into account 2ECTs, for the same device as that discussed in figure 2, but at finite temperatures. In principle, from equation (8) we learn that the Coulomb gap disappears, i.e., $V_{th}^{(n)} \to 0$, at any finite temperature (curve 2 for $T = 0.007$ and curve 3 for $T = 0.015$). In practice, if the temperature is still low enough relative to the charging energy, the current reduces very quickly with decreasing bias voltage V and may become too small to be detected at even a finite V. For example, for curve 2 with temperature $T = 0.007$ the current decreases from $\approx 1.4 \times 10^{-5}$ at $V = 0.12$ to $\approx 3.5 \times 10^{-12}$ at $V = 0.06$. At low biases the current is very sensitive to temperature, and the lower the bias, the stronger the effect of temperature on the current magnitude becomes. For STs, the finite temperature effect has been in detail discussed in [22, 25].

5. Conclusion

We have studied the tunnelling transport through an MDQDS in the regime when the conduction is essentially dominated by the SE and the lowest-order 2ECT process. Though

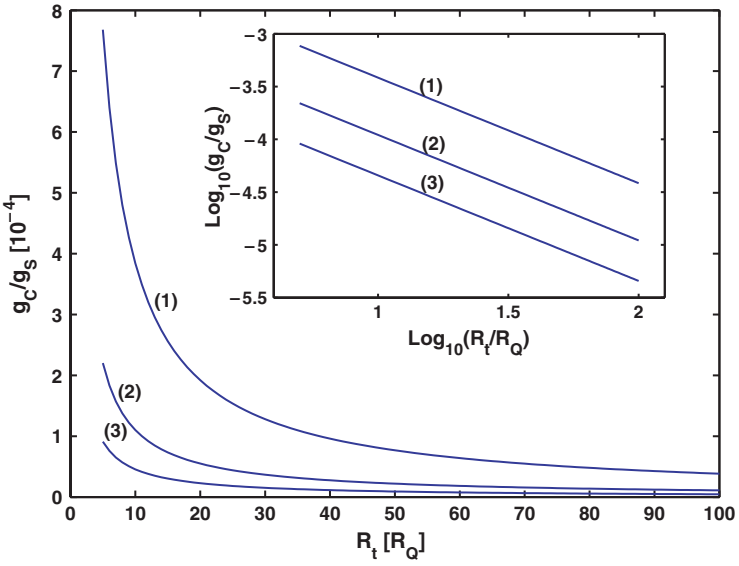

Figure 5. The ratio of the two conductances, g_C/g_S, is plotted against the tunnelling resistance R_t for the device with parameters $C_l = 1$, $R_l = R_m = R_r \equiv R_t$, $C_{g1} = C_{g2} = 0.5$, $V_g = 0$, $T = 0$. The curves are different in the inter-dot capacitance: $C_m = 5$ (curve 1), 10 (curve 2), and 15 (curve 3). The inset shows that the data follow the relation $g_C/g_S \propto R_t^{-\gamma}$ well with $\gamma \approx 1$, independent of C_m.

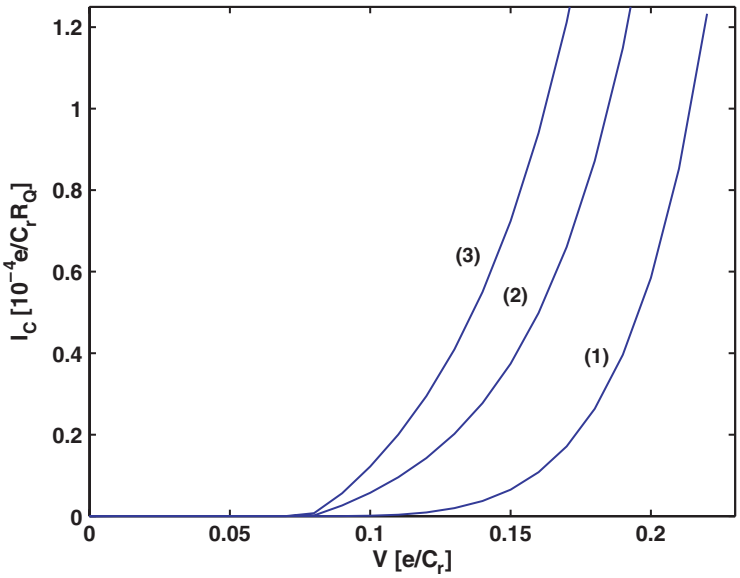

Figure 6. I–V characteristics of 2ECTs for the same device as that in figure 2, but at finite temperatures: $T = 0$ (curve 1), 0.007 (curve 2), and 0.015 (curve 3); $V_g = 0$.

the conductance of 2ECT is much smaller than that of ST, in principle, it smears the Coulomb gap, and therefore puts a limitation on the accuracy of single electron devices. It is important then to adequately evaluate the 2ECT effect (compared to STs) in devices of various parameters,

including the gate voltage. To do this, we have quantitatively examined in detail both tunnelling processes, ST and 2ECT, using the standard ME approach.

In the simple case of zero gate voltage we were able to derive analytical expressions of two threshold voltages, $V_{\rm th}^{(s)}$ for ST and $V_{\rm th}^{(2)}$ for 2ECT, with their dependence on device parameters. The ratio $V_{\rm th}^{(2)}/V_{\rm th}^{(s)}$, describing the relative role of 2ECT, decreases with increasing the inter-dot coupling capacitance C_m.

Taking into account the gate voltage $V_{\rm g}$ we have numerically solved the ME and calculated the I–V characteristics of both ST and 2ECT for devices of various parameters. The obtained results show that, while the ratio $V_{\rm th}^{(2)}/V_{\rm th}^{(s)}$ still decreases with increasing C_m, it oscillates as $V_{\rm g}$ varies. Analysing the conductance spectroscopy we found not only the well-known oscillation of the ST conductance, but also an oscillation of the 2ECT conductance in an ST-blocked region. In comparison with the ST conductance, 2ECT conductance peaks are much lower in height (by about three orders of magnitude) and the peak spacing distribution is very non-regular. The ME also allows us to calculate the I–V characteristics at finite temperature. While, in principle, both threshold voltages should vanish at any non-zero temperature, the 2ECT current seems to be more sensitive to the temperature at lower bias.

All numerical data reported can be reproduced, using Monte Carlo simulations. Actually, such simulations have been performed and we believe that in all cases of interest the two methods, ME and Monte Carlo simulation, give practically the same results.

Acknowledgments

One of the authors (VLN) thanks Professor Georg Bock for his kind hospitality at IWR (Universitat Heidelberg) where parts of this work have been done. This work was supported in part by the Fundamental Research Program from the Ministry of Science and Technology (Vietnam) and by the VAST research grant on simulation of nano-devices.

Appendix

Taking into account both tunnelling processes, STs and 2ECTs, the ME equation reads

$$\begin{aligned}\frac{\mathrm{d}}{\mathrm{d}t}p(n_i,m_i) &= \Gamma_l^+ p(n_i-1,m_i) + \Gamma_l^- p(n_i+1,m_i) + \Gamma_m^+ p(n_i+1,m_i-1)\\ &+ \Gamma_m^- p(n_i-1,m_i+1) + \Gamma_r^+ p(n_i,m_i+1) + \Gamma_r^- p(n_i,m_i-1)\\ &+ \Gamma_{lm}^{++} p(n_i,m_i-1) + \Gamma_{lm}^{--} p(n_i,m_i+1) + \Gamma_{mr}^{++} p(n_i+1,m_i)\\ &+ \Gamma_{mr}^{--} p(n_i-1,m_i) + \Gamma_{lr}^{++} p(n_i-1,m_i+1) + \Gamma_{lr}^{--} p(n_i+1,m_i-1)\\ &+ \Gamma_{lr}^{+-} p(n_i-1,m_i-1) + \Gamma_{lr}^{-+} p(n_i+1,m_i+1)\\ &- [\Gamma_l^+ + \Gamma_l^- + \Gamma_m^+ + \Gamma_m^- + \Gamma_r^+ + \Gamma_r^- + \Gamma_{lm}^{++} + \Gamma_{lm}^{--} + \Gamma_{mr}^{++} + \Gamma_{mr}^{--}\\ &+ \Gamma_{lr}^{++} + \Gamma_{lr}^{--} + \Gamma_{lr}^{+-} + \Gamma_{lr}^{-+}]p(n_i,m_i).\end{aligned}$$

This equation can be rewritten in the matrix form

$$\frac{\mathrm{d}}{\mathrm{d}t}\hat{p} = \hat{M}\hat{p}, \tag{16}$$

where $\hat{p}$ is the matrix of elements $p_i \equiv p(n_i,m_i)$ and the evolution matrix $\hat{M}$ has diagonal elements

$$\begin{aligned}M(i,i) = &-\Gamma_l^+(i) - \Gamma_l^-(i) - \Gamma_m^+(i) - \Gamma_m^-(i) - \Gamma_r^+(i) - \Gamma_r^-(i) - \Gamma_{lm}^{++}(i)\\ &- \Gamma_{lm}^{--}(i) - \Gamma_{mr}^{++}(i) - \Gamma_{mr}^{--}(i) - \Gamma_{lr}^{++}(i) - \Gamma_{lr}^{--}(i) - \Gamma_{lr}^{+-}(i) - \Gamma_{lr}^{-+}(i)\end{aligned}$$

where, for short, $\Gamma(n_i, m_i)$ is written as $\Gamma(i)$, and non-diagonal elements

$$M(i,j) = \begin{cases} \Gamma_l^+(j) + \Gamma_{rm}^{--}(j) & \text{if } n_j = n_i - 1, m_j = m_i \\ \Gamma_l^-(j) + \Gamma_{mr}^{++}(j) & \text{if } n_j = n_i + 1, m_j = m_i \\ \Gamma_m^-(j) + \Gamma_{lr}^{--}(j) & \text{if } n_j = n_i + 1, m_j = m_i - 1 \\ \Gamma_m^-(j) + \Gamma_{lr}^{++}(j) & \text{if } n_j = n_i - 1, m_j = m_i + 1 \\ \Gamma_r^+(j) + \Gamma_{lm}^{--}(j) & \text{if } n_j = n_i, m_j = m_i + 1 \\ \Gamma_r^-(j) + \Gamma_{lm}^{++}(j) & \text{if } n_j = n_i, m_j = m_i - 1 \\ \Gamma_{lr}^{+-}(j) & \text{if } n_j = n_i - 1, m_j = m_i - 1 \\ \Gamma_{lr}^{-+}(j) & \text{if } n_j = n_i + 1, m_j = m_i + 1 \end{cases}$$

where the ST and 2ECT rates are respectively defined in equation (4) or (5) and equation (7) or (8).

References

[1] For a review, see Grabert H and Devoret M H (ed) 1991 *Single Charge Tunneling* (*NATO ASI Series B*) (New York: Plenum)
[2] Averin D V and Likharev K K 1991 *Mesoscopic Phenomena in Solids* ed B L Altshuler, P A Lee and R A Webb (Amsterdam: North-Holland)
[3] Averin D V and Nazarov Yu V 1991 *Single Charge Tunneling* (*NATO ASI Series B*) ed H Grabert and M H Devoret (New York: Plenum) p 217
[4] Schoeller H and Schon G 1994 *Phys. Rev.* B **50** 18436
[5] Geerligs I J, Averin D V and Mooij J E 1990 *Phys. Rev. Lett.* **65** 3037
[6] Hanna A E, Tuominen M T and Tinkham M 1992 *Phys. Rev. Lett.* **68** 3228
[7] Eiles T M, Zimmerli G, Jensen H D and Martinis J M 1992 *Phys. Rev. Lett.* **69** 148
[8] Pasquier C, Meirav U, Williams F I B, Glattli D C, Jin Y and Etienne B 1993 *Phys. Rev. Lett.* **70** 69
[9] Cronenwett S M, Patel S R, Marcus C M, Campman K and Gossard A C 1997 *Phys. Rev. Lett.* **79** 2312
[10] De Franceschi S, Sasaki S, Elzerman J M, van der Wiel M G, Tarucha S and Kouwenhoven I P 2001 *Phys. Rev. Lett.* **86** 878
[11] DiVincenzo D P 2005 *Science* **309** 2173
[12] Yin S, Sun Q F, Sun Z Z and Wang X R 2005 *J. Phys.: Condens. Matter* **17** L183
[13] Storcz M J, Hartmann U, Kohler S and Wilhelm F K 2005 *Phys. Rev.* B **72** 235321
[14] Petta J R *et al* 2005 *Science* **309** 2180
[15] Engel H-A and Loss D 2002 *Phys. Rev* B **65** 195321
[16] van der Wiel W G, de Franceschi S, Elzerman J M, Fujisawa T, Tarucha S and Kouwenhoven L P 2003 *Rev. Mod. Phys.* **75** 1
[17] Galpin M R, Logan D E and Krishnamurthy H R 2005 *Phys. Rev. Lett.* **94** 186406
[18] Apel V M, Davidovich M A, Chiappe G and Anda E V 2005 *Phys. Rev.* B **72** 125302
[19] Bakhvalov N S, Kazacha G S, Likharev K K and Serdyukova S D 1989 *Sov. Phys.—JETP* **68** 581
[20] Sasaki S *et al* 2000 *Nature* **405** 764
[21] Tanaka Y and Kawakami N 2005 *Phys. Rev.* B **72** 085304
[22] Nguyen V H, Nguyen V L and Nguyen H N 2005 *J. Phys.: Condens. Matter* **17** 1157
[23] Nguyen V H, Nguyen V L and Dollfus P 2005 *Appl. Phys. Lett.* **87** 123107
[24] Berven C A and Wybourne M N 2001 *Appl. Phys. Lett.* **78** 3893
[25] Nguyen V L, Nguyen T D and Nguyen H N 2001 *Phys. Lett.* A **291** 150